Clinical Cancer Research

TP53, STK11, and *EGFR* Mutations Predict Tumor Immune Profile and the Response to Anti–PD-1 in Lung Adenocarcinoma

Jérôme Biton[1,2,3], Audrey Mansuet-Lupo[1,2,3,4], Nicolas Pécuchet[5,6], Marco Alifano[7], Hanane Ouakrim[1,2,3], Jennifer Arrondeau[8], Pascaline Boudou-Rouquette[8], François Goldwasser[2,8], Karen Leroy[2,9], Jeremy Goc[1,2,3], Marie Wislez[3,10], Claire Germain[1,2,3], Pierre Laurent-Puig[2,5,6], Marie-Caroline Dieu-Nosjean[1,2,3], Isabelle Cremer[1,2,3], Ronald Herbst[11], Hélène Blons[2,5,6], and Diane Damotte[1,2,3,4]

Abstract

Purpose: By unlocking antitumor immunity, antibodies targeting programmed cell death 1 (PD-1) exhibit impressive clinical results in non–small cell lung cancer, underlining the strong interactions between tumor and immune cells. However, factors that can robustly predict long-lasting responses are still needed.

Experimental Design: We performed in-depth immune profiling of lung adenocarcinoma using an integrative analysis based on immunohistochemistry, flow-cytometry, and transcriptomic data. Tumor mutational status was investigated using next-generation sequencing. The response to PD-1 blockers was analyzed from a prospective cohort according to tumor mutational profiles and PD-L1 expression, and a public clinical database was used to validate the results obtained.

Results: We showed that distinct combinations of *STK11*, *EGFR*, and *TP53* mutations were major determinants of the tumor immune profile (TIP) and of the expression of PD-L1 by malignant cells. Indeed, the presence of *TP53* mutations without co-occurring *STK11* or *EGFR* alterations (*TP53*-mut/*STK11-EGFR*-WT), independently of *KRAS* mutations, identified the group of tumors with the highest CD8 T-cell density and PD-L1 expression. In this tumor subtype, pathways related to T-cell chemotaxis, immune cell cytotoxicity, and antigen processing were upregulated. Finally, a prolonged progression-free survival (PFS: HR = 0.32; 95% CI, 0.16–0.63, $P < 0.001$) was observed in anti–PD-1-treated patients harboring *TP53*-mut/*STK11-EGFR*-WT tumors. This clinical benefit was even more remarkable in patients with associated strong PD-L1 expression.

Conclusions: Our study reveals that different combinations of *TP53*, *EGFR*, and *STK11* mutations, together with PD-L1 expression by tumor cells, represent robust parameters to identify best responders to PD-1 blockade. *Clin Cancer Res; 24(22); 5710–23. ©2018 AACR.*

Introduction

The landscape of cancer therapy is currently being transformed by the recent clinical success of immunotherapies, and more particularly of those targeting the so-called immune checkpoints (ICP; refs. 1–3). In non–small cell lung cancer (NSCLC), antibodies targeting programmed cell death 1 (PD-1) have shown unprecedented durable clinical responses, even in patients with advanced metastatic disease (4, 5). Unfortunately, only a subgroup of patients had long-lasting responses, highlighting the urgent need to identify biomarkers that will robustly predict the effectiveness of ICP blockade. To efficiently predict clinical response to ICP inhibitors and to be routinely used in clinical practice, these biomarkers will have to meet two main criteria: a reliable and precise identification of responders and nonresponders, associated with an acceptable technical feasibility in terms of time and of cost.

In the field of oncoimmunology, extensive efforts have been made recently to identify predictive markers of the therapeutic response to anti–PD-1-targeted therapies. Several markers had

[1]Institut National de la Santé et de la Recherche Médicale (INSERM), UMRS 1138, Cordeliers Research Center, Team Cancer, Immune Control and Escape, Paris, France. [2]University Paris Descartes, Paris, France. [3]University Pierre et Marie Curie-Paris, Paris, France. [4]Department of Pathology, Assistance Publique, Hôpitaux de Paris (APHP), Hôpital Cochin, Paris, France. [5]INSERM UMRS 1147, Paris, France. [6]Department of Biochemistry, APHP, Hôpital Européen Georges Pompidou, Paris, France. [7]Department of Thoracic Surgery, APHP, Hôpital Cochin, Paris, France. [8]Department of Medical Oncology, APHP, Hôpital Cochin, Paris, France. [9]Department of Genetic and Molecular Biology, APHP, Hôpital Cochin, Paris, France. [10]Department of Respiratory Medicine, APHP, Hôpital Tenon, Paris, France. [11]Oncology Research, MedImmune, LLC, Gaithersburg, Maryland.

Note: Supplementary data for this article are available at Clinical Cancer Research Online (http://clincancerres.aacrjournals.org/).

Current address for J. Biton: INSERM, UMR 1125, Bobigny, France, or Sorbonne Paris Cité Université Paris 13, Bobigny, France; and current address for J. Goc, Joan and Sanford I. Weill Department of Medicine, Division of Gastroenterology and Hepatology, Department of Microbiology and Immunology and Jill Roberts Institute for Research in Inflammatory Bowel Disease, Weill Cornell Medicine, Cornell University, New York, NY 10065.

Corresponding Author: Diane Damotte, INSERM, UMRS 1138, Cordeliers Research Center, Team Cancer, Immune Control and Escape, 15 rue de l'école de Médecine, F-75006, Paris, France. Phone: 33-1-44-27-90-86; Fax: 33-1-44-27-81-17; E-mail: diane.damotte@aphp.fr

doi: 10.1158/1078-0432.CCR-18-0163

©2018 American Association for Cancer Research.

Downloaded from http://aacrjournals.org/clincancerres/article-pdf/24/22/5710/2049288/5710.pdf by guest on 10 January 2023

Translational Relevance

Antibodies targeting the PD-1/PD-L1 pathway brought an unprecedented hope to cure lung cancer. However, complete responses are seen in a minority of patients and are still not completely predictable. Recently proposed predictive biomarkers encountered multiple challenges, including imperfect identification of responders, and/or limited technical feasibility. We found that distinct combinations of *STK11*, *EGFR*, and *TP53* mutations, independently of *KRAS* alterations, were associated with different tumor microenvironments in terms of immune cell composition and of PD-L1 expression by tumor cells. Indeed, the presence of *TP53* mutations without alterations in *STK11* or in *EGFR* genes designated tumors with the strongest adaptive immune response together with the presence of tumor immune evasion, and thus allowed identification of patients with the highest sensitivity to anti–PD-1 therapies. Our study provides evidence that routine next-generation sequencing of three commonly mutated genes, together with the evaluation of PD-L1 expression, represents robust biomarkers to identify best responders to PD-1 blockade.

been proposed, including tumor mutational burden (TMB; ref. 6), DNA mismatch-repair deficiency (7), PD-L1 expression by tumor cells (4, 5, 8), and gene signature reflecting preexisting adaptive immunity (9, 10). Nevertheless, the implementation of predictive parameters like immune gene signatures and TMB requires reliable but expensive genomic platforms, in addition to heavy whole exome sequencing (WES) experiments in the case of TMB analysis. To bypass these limitations, novel methods have been developed to predict TMB from targeted cancer gene next-generation sequencing panels. However, in order to be accurate, and properly correlated to WES, it was shown that gene panels needed to encompass at least 1 to 2 Mb (11, 12). The expression of PD-L1 by tumor cells currently used to predict the response to PD-1 blockade, also encounters several issues. These include the lack of consensus regarding the anti-PD-L1 antibodies used in IHC, the threshold used to determine the positivity during quantification, and the potential discrepancies between primary and metastatic biopsies stained. Additionally, only a fraction of tumors expressing PD-L1 respond to PD-1 inhibition. Oncogenic pathways (13) versus immune-induced PD-L1 expression (14) may account for the latter point. Importantly, the main limitation of such strategy is linked to the choice of an optimal cutoff for clinical decision making. Indeed, currently, tumors below this cutoff may respond to anti–PD-1, although this is less likely. To overcome these obstacles, and considering that oncogenic drivers (*EGFR* and *KRAS*) and mutations in tumor suppressor genes (*TP53* and *STK11*) may have a major impact on the immune microenvironment of lung tumors (15–17), a recent study reported increased sensitivity to PD-1 blockade in patients with *TP53* and/or *KRAS* mutations (18). However, not all patients with *TP53* and/or *KRAS*-mutated tumors responded to this ICP blockade (18). Common to these different strategies for patient selection is the aim to identify tumors that show the presence of an adaptive immune response, together with upregulation of mechanisms of immune evasion, such as expression of PD-L1 (6, 7, 10, 15, 18). Therefore, the identification of even more accurate predictive markers probably involves a better understanding of mechanisms involved in the shaping of the tumor immune microenvironment.

In this context, to study the interplay between malignant cells and their immune microenvironment, we performed from lung adenocarcinoma samples an integrative analysis that incorporated IHC, gene expression, mutational and flow-cytometry data. We identified three main tumor immune profiles (TIP) and found that co-occurring genetic alterations, especially *TP53*, *EGFR*, and *STK11* mutations, are major determinants of the tumor immune composition and of PD-L1 expression by malignant cells. Moreover, we found that distinct combinations of *TP53*, *EGFR*, and *STK11* mutations were able to identify best responders to PD-1 blockers.

Materials and Methods

Cohorts

A retrospective consecutive cohort of 221-untreated patients with primary lung adenocarcinoma seen between June 2001 and December 2005 at the department of Thoracic Surgery of Hôtel-Dieu hospital (Paris, France) was used to study by IHC the immune composition of the tumor microenvironment. All patients underwent complete surgical resection of their tumor. The second cohort was a consecutive selection of 24 patients with untreated primary lung adenocarcinoma who underwent surgery between March 2015 and June 2017 and for whom fresh tumor samples were obtained. These samples were used to perform flow-cytometry experiments. The third cohort was composed of 32 advanced-stage lung adenocarcinoma patients enrolled by the Cochin Immunomodulatory Therapies Multidisciplinary Study group (CERTIM) from February 2015 through August 2016 and treated with nivolumab (anti–PD-1, Bristol Myers Squibb) at a dose of 3 mg per kilogram of body weight every 2 weeks. RECIST 1.1 criteria were used to monitor response to nivolumab. Written informed consent was obtained from all patients. The protocol was approved by the local ethics committee (CPP Ile de France II, no. 2008-133, and 2012 06-12) in agreement with article L.1121-1 of French law. Additional details are provided in the Supplementary Methods.

Clinical and mutational data from 31 NSCLC patients treated with pembrolizumab (anti–PD-1, Merck) were collected from cbioPortal (http://www.cbioportal.org/study?id=luad_mskcc_2015#summary). Additional details are provided in the Supplementary Methods.

IHC and cell quantification

Formalin-fixed, paraffin-embedded (FFPE) lung tumor samples were selected and stained as previously described (19, 20) using polyclonal anti-CD3 (Dako), anti–MHC-I (EMR8-5, Abcam), anti-CD8 (SP16, Spring-Bioscience), anti–DC-Lamp (1010.01, Dendritics), anti-CD66b (G10F5, BD Biosciences), anti–PD-L1 (E1L3N, Cell Signaling Technology) or anti-CD68 (PG-M1, Dako). Calopix software (Tribvn) was used to count $CD66b^+$ and $CD68^+$ cells in the whole tumor section; CD8 T cells were counted separately in the tumor nests and in tumor stroma. DC-$Lamp^+$ cells were counted manually in the whole tumor section. Areas of the whole tumor section, tumor nests, and tumor stroma were determined by using Calopix software. For $CD66b^+$, $CD68^+$, $CD8^+$, and DC-$Lamp^+$ cells, results are expressed as absolute number of positive cells/mm^2. The proportion of

Downloaded from http://aacrjournals.org/clincancerres/article-pdf/24/22/5710/2049288/5710.pdf by guest on 10 January 2023

MHC-I$^+$ and PD-L1$^+$ cells among tumor cells was determined manually by at least two independent observers (J. Biton, A. Mansuet-Lupo, or D. Damotte). The positivity threshold was fixed at $\geq$1%. Additional details are provided in the Supplementary Methods.

Molecular analysis

DNA was extracted from FFPE tumor samples selected based on the highest percentage of tumor cells, using the illustra Nucleon BACC2 genomic DNA extraction kit (GE Healthcare Life Sciences). In the retrospective cohort of 221 lung adenocarcinoma, samples were characterized using NGS and a custom AmpliSeq panel (AmpliSeq Ion Torrent; Life Technologies) that included *EGFR* (exons 18–21), *TP53* (exons 2–11), *KRAS* (exons 2–6), *BRAF* (exons 11–15), *NRAS* (exons 2–5), *HER2* (exons 18–21), and *STK11* (exons 1–9) as previously described (19). In the prospective cohort of 24 lung adenocarcinoma and in the CERTIM cohort, samples were characterized using Ion AmpliSeq Colon and Lung Cancer Research Panel v2 that included 22 mutations (for more details see manufacturer's notice; Thermo Fisher Scientific). The sequencing reads were processed using Ion Torrent Suite V4.0 software (Life Technologies). Regarding the classification of *TP53*, *STK11*, and *EGFR* mutation subtypes, additional details are provided in the Supplementary Methods.

Flow cytometry

Multiple stainings on isolated mononuclear cells from tumors were performed using various antibodies (see Supplementary Table S1), as previously described (21). Additional details are provided in the Supplementary Methods.

NanoString-based gene expression profiling

Total RNA was isolated from FFPE tumor samples using the Recover All Total Nucleic Acid Isolation Kit (Invitrogen) according to the manufacturer's protocol. The RNA concentration and purity was estimated on NanoDrop 2000 spectrophotometer (Thermo Fisher Scientific). NanoString Technologies-based gene expression profiling was performed on 50 ng of total RNA from each sample according to the manufacturer's instructions. Tumor RNA samples were subjected to analysis by nCounter PanCancer Immune Profiling Panel (NanoString Technologies) consisting of 770 human genes. The mRNA hybridization, detection, and scanning were realized following the NanoString protocol. Normalization of raw data was performed using the nSolver software (NanoString Technologies) based on the 10 most relevant housekeeping genes. Heatmaps were generated with Genesis software (Institute of Genomics and Bioinformatics).

Statistical analysis

Categorical data were compared using χ^2 test or Fisher exact test, as appropriate. In flow cytometry experiments, according to data distribution, a parametric test (ANOVA, Student *t* test) or a nonparametric test (Kruskal–Wallis, Mann–Whitney), with appropriate *post hoc* comparisons was used. Regarding NanoString analysis, the normalized mRNA counts were log-transformed and a two-tailed *t* test was performed to compare gene expression. False discovery rates (FDR) were calculated using the Benjamini–Hochberg procedure. Survival analyses were made using both the log-rank test and a Cox proportional-hazard regression model. The start of follow-up for overall survival (OS) was the time of surgery (221 lung adenocarcinoma cohort) or the time of first anti–PD-1 injection (CERTIM cohort). The start date of follow-up for progression-free survival (PFS) was the time of first anti–PD-1 injection (CERTIM cohort). For Cox proportional-hazard regression model, immune cell densities were log transformed. Analyses were made using GraphPad Prism, Statview (Abacus Systems) and R (http://www.r-project.org/) software.

Results

Immune cell densities clustering defines three distinct TIPs

To determine whether lung adenocarcinomas could be classified according to their TIPs, we first used a retrospective cohort of 221 patients. By IHC, we determined in each tumor, the densities of neutrophils (CD66b$^+$ cells), macrophages (CD68$^+$ cells), CD8 T cells in the tumor nests (CD8$_{Tu}$), and in the stroma (CD8$_s$), and of mature DCs (DC-Lamp$^+$ cells) reflecting the presence of tertiary lymphoid structures (Fig. 1A–D; ref. 22). As expected, the strongest correlations were observed between CD8$_{Tu}$ cell and CD8$_S$ cell densities, followed by that between DC-Lamp$^+$ cell and CD8$_S$ cell densities (Supplementary Fig. S1). Then, we performed hierarchical clustering of immune cell densities to determine whether tumor could be classified more precisely according to their immune profiles. We identified three distinct TIPs (Fig. 1E). The first one (TIP-1) was characterized by the highest density of CD8 T cells, indicating a strong adaptive immune response (Fig. 1E, I, and J). The main feature of TIP-2 was a strong infiltration of macrophages (Fig. 1E and G). In TIP-3, most tumors could be classified as immunologically ignored, although some of them exhibited a high density of neutrophils (Fig. 1E and F–J). Moreover, the clinical parameters did not differ among the TIPs except an increased proportion of male in the TIP-1 (Supplementary Table S2). Interestingly, TIP-1 was also composed of two subgroups, TIP-1a and TIP-1b, which mainly differed regarding CD8$_{Tu}$ cell density, with the highest density of CD8$_{Tu}$ cells observed in TIP-1b (Supplementary Fig. S2A–S2E).

PD-L1 expression affects patients' survival only in TIP-1

In NSCLC, previous works have reported an association between patient survival and the immune composition of tumors (20, 21). In this study, patient OS was not significantly different among TIP-1, TIP-2, and TIP-3 (Fig. 2A). Even when TIP-2 and TIP-3 were combined, only a nonsignificant trend toward a longer OS in TIP-1 was observed (Fig. 2B). Moreover, OS was not significantly different between patients belonging to TIP-1a and TIP-1b (Supplementary Fig. S2F). Together, these results suggested that tumor burden control by CD8 T cells, especially in TIP-1, could be altered by the development of mechanisms allowing tumor to escape immune surveillance. The most-studied mechanism being PD-L1 expression by tumor cells, we then investigated whether different levels of PD-L1 expression by tumor cells in the three TIPs could explain this absence of significant differences in terms of OS (Fig. 2C–E). The mean percentages of PD-L1$^+$ tumor cells were higher in the TIP-1 group (Fig. 2F). Similarly, when applying a threshold of positivity $\geq$1%, the proportion of PD-L1$^+$ tumors was higher in the TIP-1 group (Fig. 2F). Interestingly, the frequency of PD-L1$^+$ tumors was even more increased in the TIP-1b compared with the TIP-1a group (Supplementary Fig. S2G). Univariate Cox-regression analysis showed a negative prognostic value for PD-L1 expression by tumor cells only in TIP-1 (Fig. 2G).

Downloaded from http://aacrjournals.org/clincancerres/article-pdf/24/22/5710/2049288/5710.pdf by guest on 10 January 2023

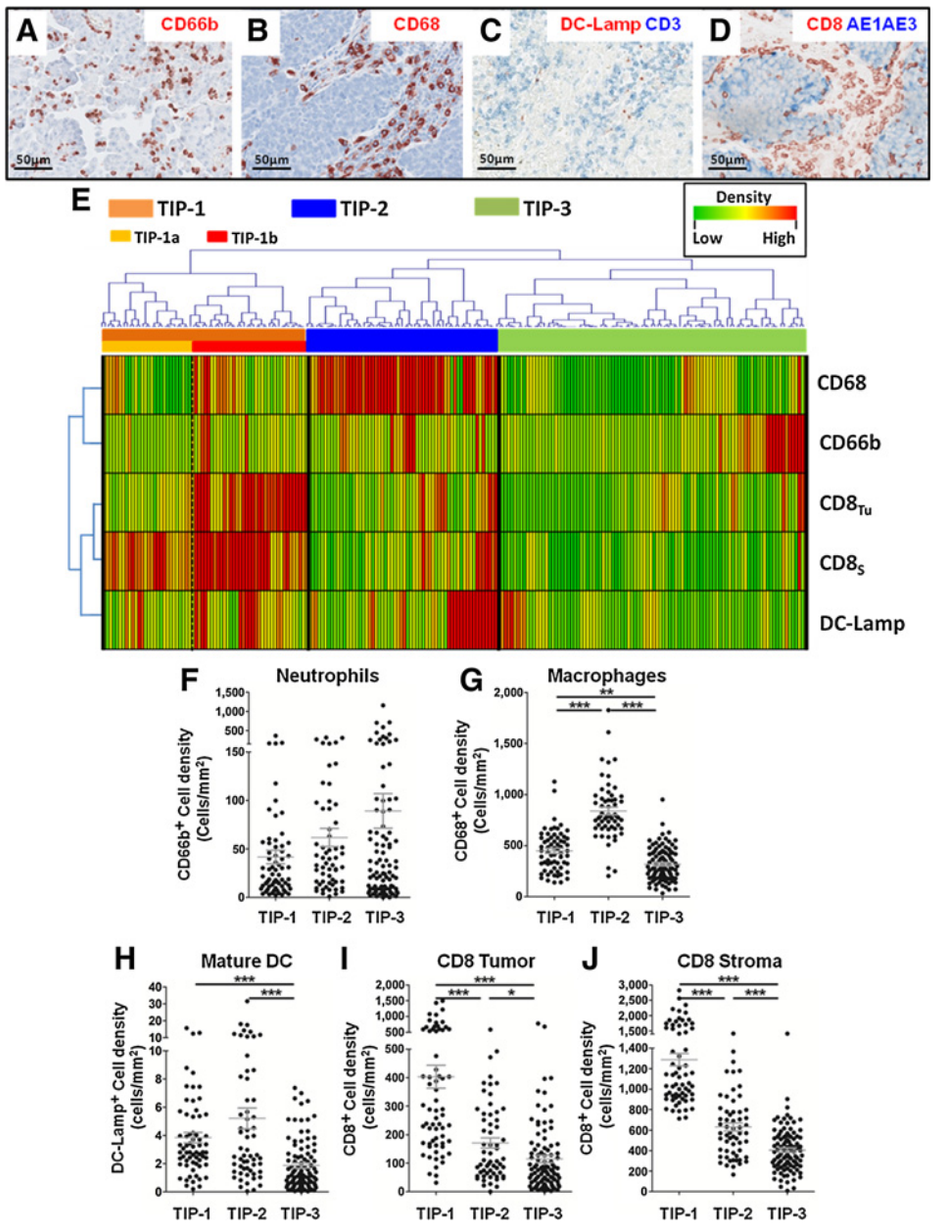

Figure 1.
Identification of three distinct TIPs in a retrospective cohort of lung adenocarcinoma. **A** and **B,** $CD66b^+$ cells (red cells in **A**) and $CD68^+$ cells (red cells in **B**) were counted in the whole tumor section. **C,** Tertiary lymphoid structures (TLS) are composed of T-cell–rich areas comprising DC-$Lamp^+$ DCs (in red) forming clusters with $CD3^+$ T cells (in blue). DC-$Lamp^+$ cells were counted in the whole tumor section. **D,** $CD8^+$ T cells (red cells) were counted selectively in pan-$cytokeratin^+$ tumor nests (blue cells) stained with AE1/AE3 and in the stroma. **E,** Immune cell densities clustering from 221 lung adenocarcinomas. **F–J,** Distribution of $CD66b^+$, $CD68^+$, $CD8_{Tu}{}^+$, $CD8_S{}^+$, and DC-$Lamp^+$ cell density in the three identified TIPs. In **F–J**, data were expressed as mean and a nonparametric test (Kruskal–Wallis test followed by a *post hoc* Dunn test) was applied based on Shapiro normality test. *, $P < 0.05$; **, $P < 0.01$; and ***, $P < 0.001$.

TIPs are strongly affected by *TP53*, *STK11*, and *EGFR* mutations

The differential level of PD-L1 expression by tumor cells in the three identified TIPs might suggest that malignant cells differed at the molecular level in each TIP. To determine whether molecular alterations of tumor cells were involved in the shaping of their immune microenvironment, we investigated the distribution of 7 gene alterations in each TIP, including that of the four most common mutations in lung adenocarcinoma (*TP53*, *KRAS*, *STK11*, and *EGFR*; ref. 23). Only *TP53* and *STK11* mutations were differentially distributed in the three identified TIPs (Fig. 3A). *TP53* mutations were enriched in TIP-1 (Fig. 3A) and to an even greater extent in TIP-1b (Supplementary Fig. S2H), while *STK11* mutations were enriched in TIP-3 (Fig. 3A). Consequently, *TP53*-mutated tumors were characterized by higher CD8s densities and PD-L1 expression (Fig. 3B; Supplementary Fig. S3A). In contrast, *STK11*-mutated tumors were characterized by higher neutrophil density, lower CD8s and DC-$Lamp^+$ cell density, and lower PD-L1 expression (Supplementary Fig. S3B). *EGFR* mutations were associated with a lower amount of neutrophils, macrophages, $CD8_{Tu}$ cells, and PD-L1 expression, together with a higher mature DC density (Supplementary Fig. S3C), while *KRAS* mutations did not affect the composition of the tumor immune microenvironment.

We then investigated whether *TP53*, *STK11*, and *EGFR* mutation subtypes differed in the three TIPs (see Supplementary Methods). Most *TP53* alterations were missense mutations (Supplementary Fig. S4A), and among the three TIPs, no significant differences were observed regarding the distribution of *TP53* missense mutations, nonsense mutations, deletions resulting in frameshift and mutations in splicing sites (Supplementary Fig. S4A). Similarly, the distribution of the different types of *TP53*

Downloaded from http://aacrjournals.org/clincancerres/article-pdf/24/22/5710/2049288/5710.pdf by guest on 10 January 2023

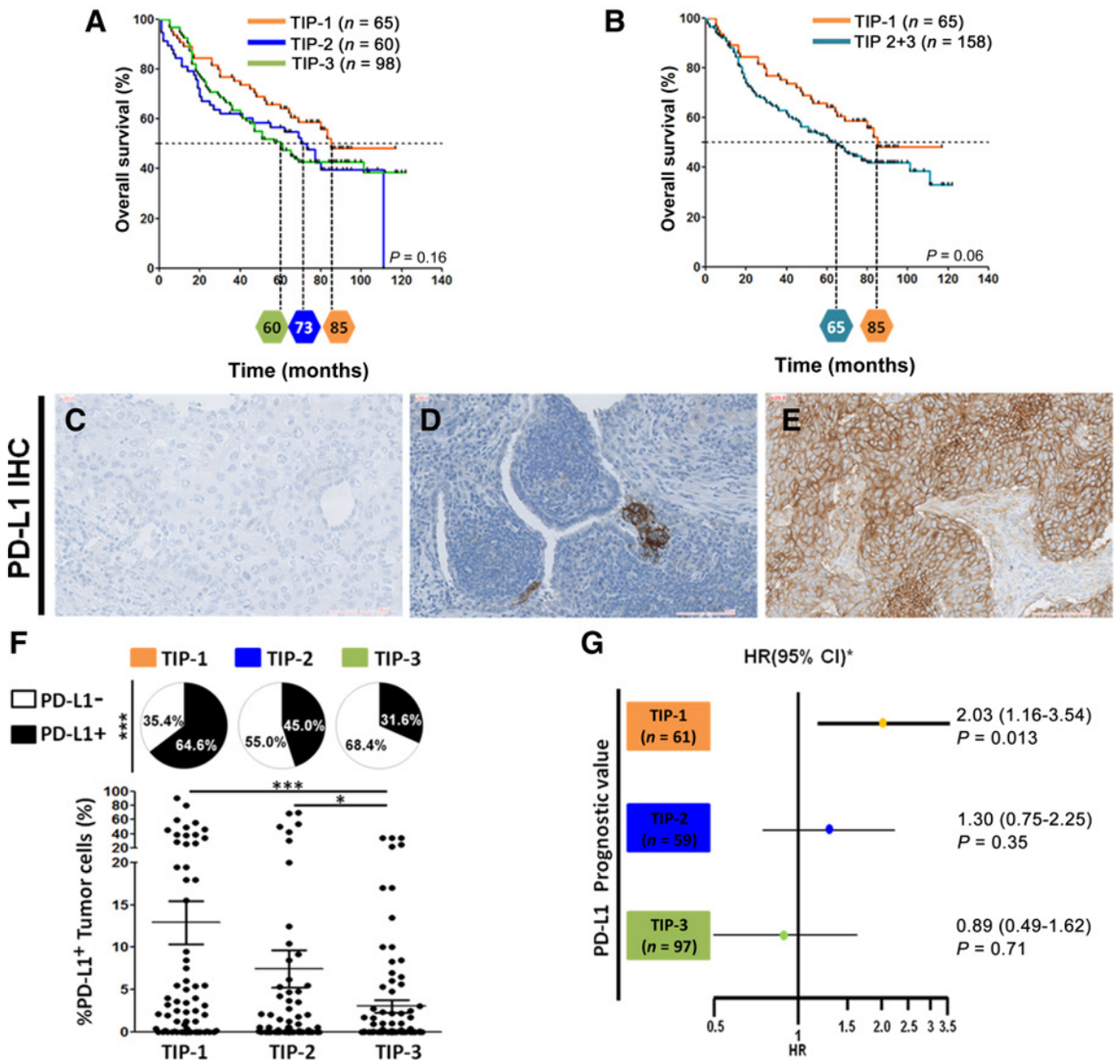

Figure 2.

Higher expression of PD-L1 by tumor cells in TIP-1 negatively affects patients' survival. **A,** Kaplan–Meier curves of OS in patients belonging to TIP-1, -2, and -3. **B,** Kaplan–Meier curves of OS in patients belonging to TIP-1 and TIP-2+3. **C–E,** Example of tumors with no expression of PD-L1 (%PD-L1$^+$ tumor cells <1%; N, negative; **C**), weak expression (%PD-L1$^+$ tumor cells ≥1% and <50%; W, weak; **D**), and strong expression (%PD-L1$^+$ tumor cells ≥50%; S, strong; **E**). **F,** PD-L1 expression by tumor cells in TIP-1 to -3. **G,** Forest plots of univariate Cox regression analysis showing the impact of PD-L1 expression by tumor cells on OS in patients belonging to TIP-1 to -3. In **A, B,** and **G,** *P* values <0.05 were considered statistically significant. In **F,** data were expressed as mean and a nonparametric test (Mann–Whitney) was applied based on Shapiro normality test. *, $P < 0.05$ and ***, $P < 0.001$.

point mutations was similar in the three TIPs (Supplementary Fig. S4B). Moreover, the proportion of each *TP53* missense mutation subtypes, classified according to their impact on the transcriptional activity of p53 (Supplementary Fig. S4C) (24), was similar among the three TIPs. Regarding *EGFR* mutations in lung cancer, deletion in exon 19 (Del 19) and L858R mutation in exon 21 represented approximately 90% of all *EGFR* alterations (25), and their proportions were not significantly different among the three TIPs, despite a trend toward an enrichment of TIP-1 in DEL19 (Supplementary Fig. S4D). Finally, *STK11* mutations can either result in a potential gain of oncogenic function (GOF) or be associated with tumor-suppressive function (TSF) (19, 26). Again, the frequencies of *STK11*-GOF and of *STK11*-TSF mutations were not significantly different in the TIP-1, TIP-2, and TIP-3, even if as opposed to TIP-2 and TIP-3, no *STK11*-GOF mutations were detected in TIP-1 (Supplementary Fig. S4). However, GOF and TSF-*STK11* mutations did not differentially affect the composition of the tumor immune microenvironment (Supplementary Fig. S4F).

TIPs are strongly influenced by distinct combinations of *TP53*, *STK11*, and *EGFR* mutations

NSCLC tumors have a high mutational burden with frequent co-occurring mutations, including co-occurring *TP53* and *STK11* mutations or *TP53* and *EGFR* mutations (27). To go further, we then investigated whether distinct combinations of *TP53*, *STK11*,

Downloaded from http://aacrjournals.org/clincancerres/article-pdf/24/22/5710/2049288/5710.pdf by guest on 10 January 2023

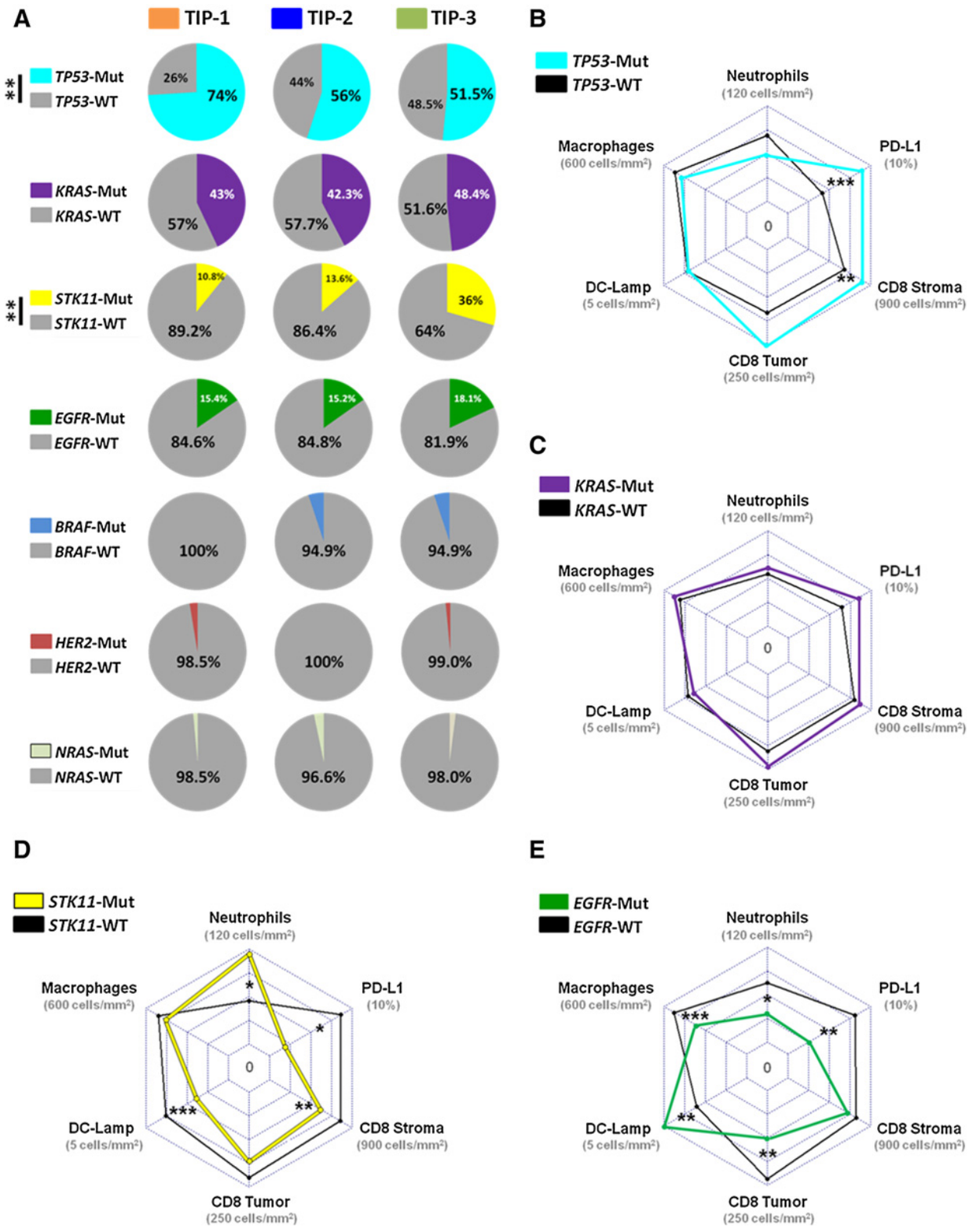

Figure 3.

Molecular alterations of tumor cells are differentially distributed in the three identified lung adenocarcinoma immune profiles. **A,** Percentages of *TP53, KRAS, STK11, EGFR, BRAF, HER2*, and *NRAS*-mutated tumors in each TIP. **B–D,** Radar plots showing the density of $CD68^+$, $CD66b^+$, $CD8_{Tu}^+$, $CD8_S^+$, and $DC\text{-}Lamp^+$ cells and the percentages of tumor cells expressing PD-L1 in *TP53*-mutated tumors (**B**), *KRAS*-mutated tumors (**C**), *STK11*-mutated tumors (**D**), and *EGFR*-mutated tumors (**E**), compared with their wild-type counterparts. In **A**, data were compared using χ^2 tests. In **B–D**, data were expressed as mean and a nonparametric test (Mann–Whitney) was applied based on Shapiro normality test. *, $P < 0.05$; **, $P < 0.01$; and ***, $P < 0.001$.

Downloaded from http://aacrjournals.org/clincancerres/article-pdf/24/22/5710/2049288/5710.pdf by guest on 10 January 2023

and *EGFR* mutations differentially affected the immune composition of the tumor microenvironment. The highest densities of $CD8_{Tu}$ and $CD8_S$ cells, together with the highest expression of PD-L1 by malignant cells, were observed in *TP53*-mutated tumors unaffected by additional *STK11* nor *EGFR* mutations (*TP53*-Mut/*STK11-EGFR*-WT; Fig. 4D–F). In the *TP53*-mutated subgroup, an additional mutation of *STK11* was significantly associated with a reduced expression of PD-L1 and a lower $CD8_S$ cell density (Fig. 4E and F). Additionally, the highest density of neutrophils was found in *STK11*-mutated tumors without mutations of *TP53* (Fig. 4A). In the two predominant groups of patients, *TP53*-Mut/*STK11-EGFR*-WT tumors ($n = 92$) and tumors without *TP53*, *STK11* nor *EGFR* mutations (*TP53-STK11-EGFR*-WT; $n = 45$), an additional alteration of *KRAS* did not affect immune cell densities nor PD-L1 expression (Supplementary Fig. S5). This result confirmed the lack of impact of *KRAS* mutations on the TIP. Remarkably, the frequency of *TP53*-Mut/*STK11-EGFR*-WT tumors was higher in TIP-1 (60%), and to a greater extent in TIP-1b (73%), than in TIP-2 (42.4%) and TIP-3 (28.8%; Fig. 4G). Finally, *STK11*-mutated tumors without *EGFR* or *TP53* alterations were nearly restricted to TIP-3.

TP53-Mut/*STK11-EGFR*-WT tumors are characterized by an upregulation of gene signatures associated with T-cell chemotaxis, cytotoxicity, and antigen presentation by MHC-I

Within a prospective cohort of 24 patients with lung adenocarcinomas, we investigated more precisely by flow cytometry whether effector functions of CD8 TILs were modified according to the tumor mutational status (Supplementary Figs. S6 and S7). In this cohort, 20 patients had at least one mutation in *KRAS*, *TP53*, *EGFR*, or *STK11*. Among them, 58% had a *KRAS* mutation, 33% a *TP53* mutation, 8% an *EGFR* mutation, and 4% a *STK11* mutation (Supplementary Fig. S7A). Importantly, among *TP53*-mutated tumors, none had an additional *STK11* or *EGFR* mutation. Based on above results, we compared CD8 TIL phenotypes between *TP53*-WT tumors and *TP53*-Mut/*STK11-EGFR*-WT tumors. Similarly, as described above, a higher $CD8_{Tu}$ cell density and PD-L1 expression by tumor cells were observed in the *TP53*-Mut/*STK11-EGFR*-WT group (Supplementary Fig. S7B–S7D). In addition, frequencies of TIM-3^+ and of granzyme-B^+ cells among CD8 TILs were higher in *TP53*-Mut/*STK11-EGFR*-WT patients as compared with the *TP53*-WT group (Supplementary Fig. S7E–S7L). A similar nonsignificant trend was observed for PD-1 expression ($P = 0.1$), but no differences regarding the percentage of IFNγ^+ cells among CD8 TILs could be observed ($P = 0.4$) (Supplementary Fig. S7E–S7L).

In the same prospective cohort, we compared gene expression profile related to the immune response in cancer between *TP53*-WT tumors and *TP53*-Mut/*STK11-EGFR*-WT tumors. Twenty-one genes were upregulated in the *TP53*-Mut/*STK11-EGFR*-WT group (fold change >2 and $P < 0.01$; Fig. 5A and B). These upregulated genes were associated with three main pathways, T-cell chemotaxis (*CCL5*, *CXCL9*, *CXCL10*, *CXCL11*, and *CXCL13*), immune cell cytotoxicity (*GNLY*, *GZMA*, *GZMB*, and *PRF1*), and a pathway related to antigen processing and peptide presentation by MHC-I (*TAP1*, *PSMB8*, *PSMB9*, *HLA-A*, and *-B*; Fig. 5C). Interestingly, a higher expression of *C1QA* and *C1QB* was found in *TP53*-Mut/*STK11-EGFR*-WT group, signaling an activation of the classical complement pathway. The expression profile of the most upregulated genes in the *TP53*-Mut/*STK11-EGFR*-WT group, meaning fold change >2 and FDR ≤ 0.1, were shown in Fig. 5D–G. To determine whether tumors from the *TP53*-Mut/*STK11-EGFR*-WT group could be more immunogenic, we evaluated by IHC on the corresponding FFPE tumor sections, MHC-I expression by malignant cells (Supplementary Fig. S8A–S8C). A higher percentage of tumor expressing MHC-I was found in the *TP53*-Mut/*STK11-EGFR*-WT group than in the *TP53*-WT group (Supplementary Fig. S8D). Moreover, MHC-I expression by malignant cells was strongly associated with a higher PD-L1 expression and a higher $CD8_{Tu}$ cell density (Supplementary Fig. S8E–S8G). These last results suggested that *TP53*-Mut/*STK11-EGFR*-WT tumors were characterized by stronger immunogenicity, which could then result in more efficient recruitment of cytotoxic CD8 TILs.

Clinical benefit to anti–PD-1 is strongly influenced by distinct combinations of *TP53*, *STK11*, and *EGFR* mutations

Based on above results, we hypothesized that the different combinations of *TP53*/*STK11*/*EGFR* mutations could be used to predict the response to anti–PD-1. In our center, the Cochin Immunomodulatory Therapies Multidisciplinary Study group (CERTIM) prospectively treated 32 patients with advanced-stage lung adenocarinoma with the anti–PD-1 antibody nivolumab. We first compared the impact of each mutation separately on patient survival within this CERTIM cohort. Only *EGFR* mutations were significantly associated with a reduced OS, while a trend toward a reduced PFS was observed in *STK11*-mutated tumors (Supplementary Fig. S9A–S9H; Table S3). We then compared the response with nivolumab in three groups of patients: *TP53*-Mut/*STK11-EGFR*-WT tumors, *TP53-STK11-EGFR*-WT tumors, and $STK11_{(or)}$*EGFR*-Mut tumors. Again, a higher percentage of tumor cells expressing PD-L1, but also a higher number of smoking pack-years were observed in patients with *TP53*-Mut/*STK11-EGFR*-WT tumors (Supplementary Table S4). Remarkably, a higher frequency of patients alive was found in the group of *TP53*-Mut/*STK11-EGFR*-WT tumors (Supplementary Table S4). Moreover, a significant longer PFS (Fig. 6A) and OS (Supplementary Fig. S10A; Table S3) were observed in patients with *TP53*-Mut/*STK11-EGFR*-WT tumors compared with those with $STK11_{(or)}$*EGFR*-Mut tumors. Importantly, in the retrospective cohort of 221 lung adenocarcinomas, meaning among patients not treated with anti–PD-1, a trend toward a reduced OS was observed in patients with *TP53*-Mut/*STK11-EGFR*-WT tumors (Supplementary Fig. S10B). To further validate the results obtained using the CERTIM cohort, we reanalyzed publicly available clinical data set used in the study performed by Rizvi and colleagues (6). A total of 31 patients with advanced NSCLC were included in our analysis and all of them had been treated with an anti–PD-1 antibody (pembrolizumab) following NCT01295827 protocol. The Rizvi cohort confirmed that the longer PFS was observed in patients with *TP53*-Mut/*STK11-EGFR*-WT tumor (Fig. 6B) and showed that the higher TMB and neoantigen burden were also found in this group (Supplementary Fig. S10C and S10D). Importantly, when the CERTIM and Rizvi cohorts were combined, a significant higher proportion of patients without progression and a longer PFS (HR = 0.32; 95% CI, 0.16–0.63, $P < 0.001$) were observed in patients belonging to the *TP53*-Mut/*STK11-EGFR*-WT tumor group as compared with the two other groups (Fig. 6C and D).

However, not all patients with *TP53*-Mut/*STK11-EGFR*-WT tumors had a durable response to PD-1 blockade. Moreover, it was suggested that tumors with co-occurring *TP53*/*KRAS* mutations showed a remarkable clinical benefit to PD-1 blockers (18). Consequently, we investigated whether an additional *KRAS*

Downloaded from http://aacrjournals.org/clincancerres/article-pdf/24/22/5710/2049288/5710.pdf by guest on 10 January 2023

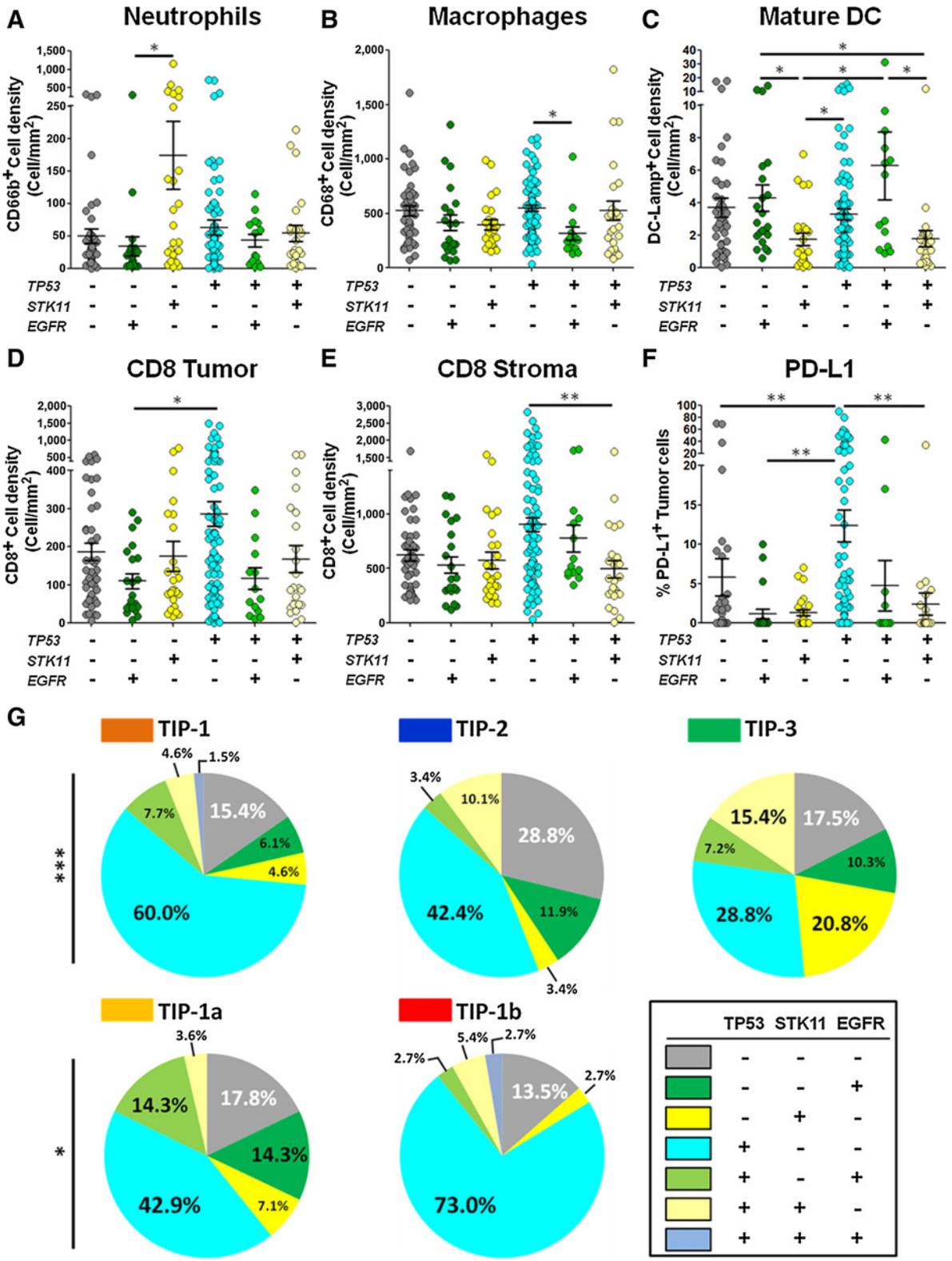

Figure 4.

Differential impact of distinct combinations of *TP53, STK11*, and *EGFR* mutations on the tumor immune composition. **A–E,** $CD66b^+$ (**A**), $CD68^+$ (**B**), DC-$Lamp^+$ (**C**), $CD8_{Tu}^+$ (**D**), and $CD8_S^+$ (**E**) cell density according to distinct combinations of *TP53, STK11*, and *EGFR* mutations. **F,** Percentage of PD-L1 expressing tumor cells according to distinct combinations of *TP53, STK11*, and *EGFR* mutations. **G,** Distribution of each combination of *TP53, STK11*, and *EGFR* mutations in each TIP. In **A–F**, data were expressed as mean and a nonparametric test (Kruskal–Wallis test followed by a *post hoc* Dunn test) was applied based on Shapiro normality test. In **G**, data were compared using χ^2 tests. *, $P < 0.05$; **, $P < 0.01$; and ***, $P < 0.001$.

Downloaded from http://aacrjournals.org/clincancerres/article-pdf/24/22/5710/2049288/5710.pdf by guest on 10 January 2023

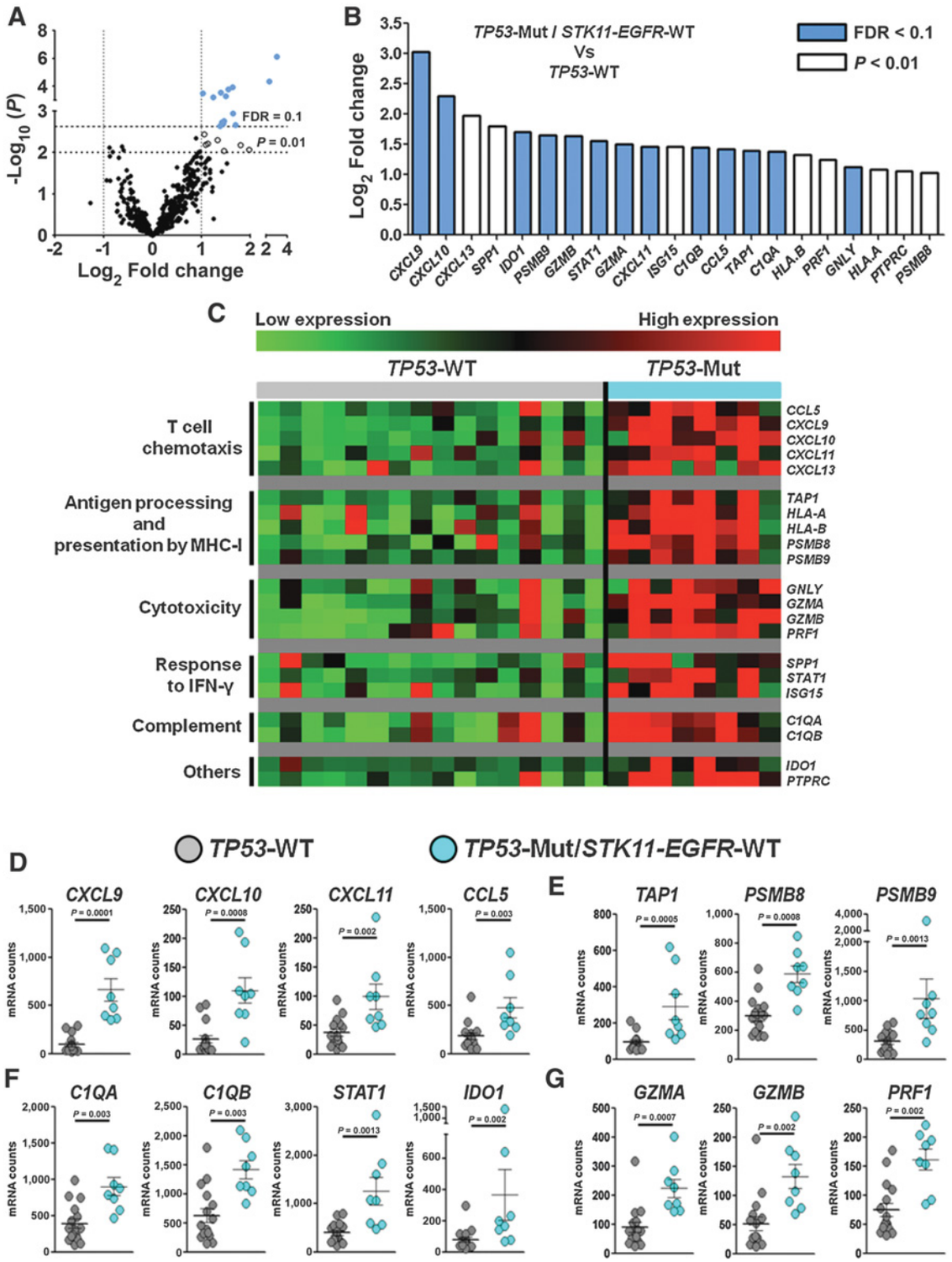

Figure 5.

Gene expression profile in *TP53*-Mut/*STK11-EGFR*-WT tumors versus *TP53*-WT tumors. **A,** Volcano plot of differentially expressed genes between *TP53*-Mut/*STK11-EGFR*-WT tumors ($n = 8$) and *TP53*-WT tumors ($n = 16$). Genes with a fold change >2 and a $P < 0.01$ (Student t test) are indicated in white circles. Genes with a fold change >2 and an FDR $\leq$0.1 (Benjamini–Hochberg correction) are indicated in blue circles. **B,** Histogram showing the $\log_2$ fold changes of the genes shown in blue and in white circles in **A**. **C,** Heatmap representation of genes differentially expressed (fold change >2 and $P < 0.01$) between *TP53*-Mut/*STK11-EGFR*-WT and *TP53*-WT tumors. **D–G,** Histograms showing the expression profile (mRNA counts) of genes most differentially expressed (fold change >2 and FDR $\leq$0.1) between *TP53*-Mut/*STK11-EGFR*-WT and *TP53*-WT tumors.

Downloaded from http://aacrjournals.org/clincancerres/article-pdf/24/22/5710/2049288/5710.pdf by guest on 10 January 2023

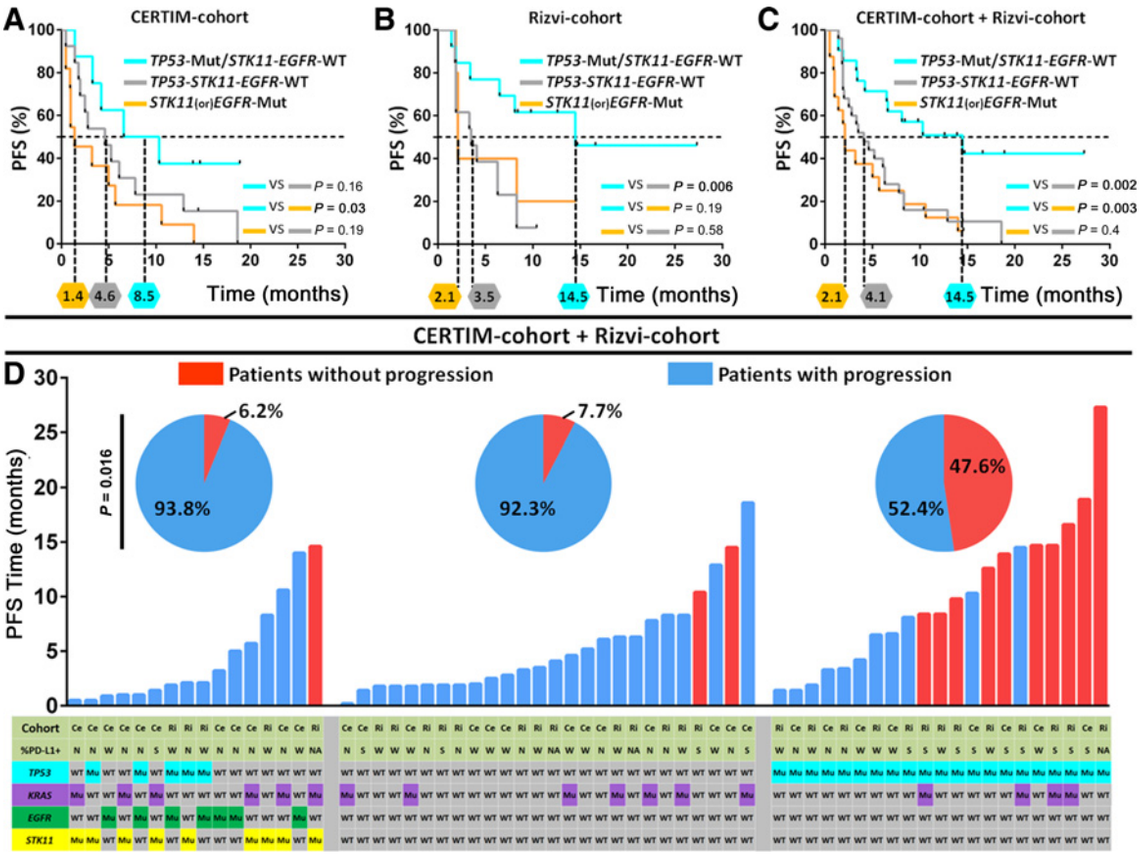

Figure 6.

Anti–PD-1 efficacy in advanced-stage NSCLC patients according to distinct combinations of *TP53, EGFR*, and *STK11* mutations. **A–C,** Kaplan–Meier curves of PFS in patients with *TP53*-Mut/*STK11-EGFR*-WT tumors, in patients with *TP53-STK11-EGFR*-WT tumors, and in patients with *STK11*$_{(or)}$*EGFR*-Mut tumors in the CERTIM cohort ($n = 8$, $n = 13$, and $n = 11$, respectively; **A**), in the Rizvi cohort ($n = 13$, $n = 13$, and $n = 5$, respectively; **B**), and in the Rizvi-cohort + CERTIM-cohort ($n = 21$, $n = 26$, and $n = 16$, respectively; **C**). **D,** Characteristics of the response to anti–PD-1 treatments according to distinct combinations of *TP53, STK11,* and *EGFR* mutations. Mu, mutated tumor; WT, wild-type tumor; NA, not available; Ce, patients from the CERTIM cohort; Ri, patients from the Rizvi cohort; PD-L1 expression: S, strong (≥50%); W, weak (≥1% and <50%); N, negative (≥50%). PFS was defined as the time from the start date of treatment to the date of the first documented event of tumor progression. Tick marks indicate censoring events. In **D**, a χ^2 test was used to compare the proportion of patients with and without progression in each group. *P* values <0.05 were considered statistically significant and appear in bold.

mutation could improve the accuracy of the identified mutational signatures to predict the response to anti–PD-1. Regarding *STK11*$_{(or)}$*EGFR*-Mut tumors, *KRAS* and *EGFR* mutations being mutually exclusive, we investigated the impact of *KRAS* only in *STK11*-Mut/*TP53-EGFR*-WT tumors. *KRAS* mutations did not affect PFS from patients having a *STK11*-Mut/*TP53-EGFR*-WT tumor, or a *TP53-STK11-EGFR*-WT tumor, while in the *TP53*-Mut/*STK11-EGFR*-WT group a nonsignificant trend toward a longer PFS was observed in patients with an additional *KRAS* alteration (Supplementary Fig. S11).

Then, we investigated whether PD-L1 expression by malignant cells could provide an additional signal to better identify patients with long-term responses. We segregated patients (CERTIM+Rizvi cohorts) according to three levels of PD-L1 expression using the methodology used in the study by Rizvi and colleagues (6), meaning no expression of PD-L1 (% of PD-L1$^+$ tumor cells <1%, N), a weak expression of PD-L1 (% of PD-L1$^+$ tumor cells ≥1% and <50%, W) and a strong PD-L1 expression (% of PD-L1$^+$ tumor cells ≥50%, S). In accordance with above results, a higher proportion of patients had a strong PD-L1 expression in the *TP53*-Mut/*STK11-EGFR*-WT group, and a longer PFS was observed in those with the highest expression of PD-L1 (Supplementary Fig. S12A and S12D). Finally, in patients with a *TP53-STK11-EGFR*-WT tumor or a *STK11*$_{(or)}$*EGFR*-Mut tumor, we did not detect any impact of PD-L1 expression by tumor cells on the PFS (Supplementary Fig. S12B and S12C).

Discussion

Our aim was to better understand the interplay between tumor cells and their immune microenvironment in order to identify new parameters able to predict the response to anti–PD-1 blockade. To achieve this objective, we first performed immune profiling of lung adenocarcinoma using an original approach, meaning unsupervised hierarchical clustering of immune cell densities. We uncovered three main TIPs, respectively characterized, by a strong CD8 T-cell density (TIP-1), a strong macrophage density (TIP-2), and a weak immune infiltrate suggesting immune

Downloaded from http://aacrjournals.org/clincancerres/article-pdf/24/22/5710/2049288/5710.pdf by guest on 10 January 2023

ignorance (TIP-3). Interestingly, we did not observe a longer OS in patients from TIP-1, suggesting that in this group, tumor control by CD8 T cells could be altered by the development of mechanisms allowing tumor to escape immune surveillance. In agreement, PD-L1 prognostic value was restricted to TIP-1, in which IFNγ secreted by TILs may have induced PD-L1 expression on tumor cells, thus allowing malignant cells to evade from the control exerted by CD8 TILs. In TIP-2 and TIP-3, PD-L1 expression was probably rather driven through oncogenic pathways (28), explaining why its impacts on patients' survival was lower. Moreover, we recently identified that CD8 TIL exhaustion was globally restricted to highly CD8 T-cell–infiltrated tumors in NSCLC (29), meaning that in TIP-1, PD-1 expression by CD8 T cells was probably higher than in TIP-2 and TIP-3. This last point might also participate in the fact that PD-L1 prognostic value was restricted to TIP-1.

Remarkably, the proportions of *TP53*-mutated and of *STK11*-mutated tumors were enriched in the TIP-1 and TIP-3 groups, respectively. The immune microenvironment of *STK11*-mutated tumors was mainly characterized by a higher density of neutrophils, a lower density of CD8 T cells in the stroma, and lower expression of PD-L1 by malignant cells. In agreement, in a *KRAS*-driven murine model of NSCLC, genetic ablation of *STK11* resulted in the accumulation of neutrophils with T-cell suppressive capacities (30). Moreover, *STK11*-mutated tumors, in murine model of NSCLC and in human cell lines, overproduced pro-inflammatory cytokines (IL6, G-CSF, and CXCL-7) which might contribute to this accumulation of neutrophils (30). Mechanisms explaining the lower expression of PD-L1 in *STK11*-mutated tumors are not fully understood. However, this point could be indirectly related to a weaker T-cell activity in *STK11*-mutated tumors, and thus to a lower amount of IFNγ secreting T cells, a cytokine known to induce PD-L1 expression (31). Concerning *TP53* alterations, mutated tumors were previously shown to be associated with an increased TMB, probably responsible for higher tumor immunogenicity, thus promoting the establishment of a strong adaptive immune response, including an active recruitment of CD8 T cells (18). The present work validated these results, and also highlighted the higher frequency of tumor cells expressing PD-L1 in *TP53*-mutated tumors. Part of the link between PD-L1 expression and *TP53* mutations was probably due to the fact that wild-type p53 protein is able to increase the expression of miR-34, an miRNA involved in the downregulation of PD-L1 expression through its binding to the 3′ untranslated regions of PD-L1 mRNA (16).

Despite their important impact on the composition of the tumor immune microenvironment, *TP53*, *STK11*, and *EGFR* mutations were not exclusive to a given TIP, and no association could be observed between the different TIPs and particular subtypes of *TP53*, *STK11*, or *EGFR* mutations. Consequently, the differential distribution of *TP53* and *STK11* mutations in the identified TIPs cannot fully explain the major differences of the tumor immune composition observed in these three groups. Therefore, we then investigated the impact of different combinations of mutations that individually affected (*TP53*, *STK11*, and *EGFR* mutations) the immune composition of the tumor microenvironment. Interestingly, we determined that *TP53*-Mut/*STK11-EGFR*-WT tumors identified a subtype of TIP (TIP-1) enriched in CD8 T cells and in malignant cells expressing PD-L1. Indeed, in *TP53*-mutated tumor, an additional *STK11* alteration was associated with a dramatic decreased of CD8 T-cell density in the stroma and of PD-L1 expression by tumor cells, indicating that for these parameters, the effects associated with *STK11* mutation dominate over those resulting from *TP53* mutation. Rather than a direct impact on the regulation of PD-L1 expression in *TP53*-mutated tumors, additional *STK11* mutations could favor the establishment of an inflammatory environment (30), less prone to recruit T cells and consequently to induce PD-L1 expression on malignant cells. Moreover, *TP53*-Mut/*STK11-EGFR*-WT tumors were associated with an immune environment characterized by the upregulation of chemokines well described to attract T cells (CXCL9, 10, and 11), together with a stronger expression of genes involved in antigen processing and MHC-I presentation, indicating higher tumors' immunogenicity. Co-occurring genetic alterations in *KRAS*-mutant lung adenocarcinoma were already shown to be associated with different tumor immune patterns, including a paucity of CD8 TILs in tumors with additional gene alterations of *STK11* compared with those with additional *TP53* mutations (15). This pioneering work of Skoulidis and colleagues (15), mostly based on gene expression experiments, is in full agreement with our results but is only partly informative due to its restricted analysis to *KRAS*-mutated tumors. This strategy had prevented Skoulidis and colleagues from observing the lack of impact of *KRAS* mutations on the immune microenvironment of lung adenocarcinoma. Moreover, *KRAS* and *EGFR* mutations being mostly mutually exclusive (32) studies performed only on *KRAS*-mutated lung adenocarcinoma could not investigate the immune microenvironment of *EGFR*-mutated tumor (15, 33). Despite work showing that *EGFR* alterations increased PD-L1 expression (34), we observed here that these mutations were prone to induce a weaker immunogenic microenvironment associated with lower expression of PD-L1. Moreover, TIP-1b was the group with the lowest percentage of *EGFR*-mutated tumors. In full agreement, a recent study reported lowest TMB in patient harboring *EGFR* mutations (18). Beyond the scope of the present work, additional dedicated studies are needed to better understand the mechanisms linking *EGFR* mutations to the presence of a particular tumor immune microenvironment, characterized by a lower amount of CD8 cells, macrophages, neutrophils, and PD-L1 expression by tumor cells, together with a higher DC-Lamp density.

KRAS alterations are the most frequent oncogenic driver mutations in NSCLC (35), but the development of targeted strategies to treat patients harboring these mutations was hampered by the phenotypic heterogeneity of *KRAS*-mutated tumors. Indeed, co-occurring alterations in *TP53*, *STK11*, and *CDKN2A/B* were shown to identify three major subgroups of *KRAS*-mutant lung adenocarcinoma with distinct biology and patterns of immune system engagement (15). Recently, a higher TMB was observed in *KRAS*-mutated tumors (18). Moreover, *TP53*/*KRAS*-comutated tumors showed a higher expression of PD-L1 and CD8a mRNA than tumors with a single mutation of *TP53* or *KRAS* (18). In our cohort of 221 lung adenocarcinomas, the composition of the tumor immune microenvironment was not affected by *KRAS* mutations, whatever the group of patients considered. The study from Dong and colleagues mentioned above (18) compared the composition of the tumor immune microenvironment of *TP53*/*KRAS*-comutated tumors to that of tumors with a single mutation of *TP53* or *KRAS*, without taking into account co-occurring *EGFR* alterations (14). As mentioned above, *EGFR* alterations reflect the presence of a tumor immune desert. Moreover, *KRAS* and *EGFR* mutations being mostly mutually exclusive, a lower proportion of *EGFR*

Downloaded from http://aacrjournals.org/clincancerres/article-pdf/24/22/5710/2049288/5710.pdf by guest on 10 January 2023

mutations in patients with co-occurring *TP53*/*KRAS* alterations as compared with tumors only mutated in *TP53* might be strongly responsible of the observed effects.

Recent studies investigated independently the impact of each mutation, meaning *EGFR*, *KRAS*, and *TP53*, on the response to PD1/PD-L1 blockade (4, 18, 36–38). We confirmed in our CERTIM cohort that the presence of *EGFR* mutations was associated with a reduced OS, but as opposed to the report of Dong and colleagues (18), we showed here that *KRAS* and *TP53* alterations separately did not statistically affect patient survival. At the time of manuscript preparation, a study performed in *KRAS*-mutant lung adenocarcinoma confirmed the lack of impact of *TP53* mutations on the survival of patients receiving an anti–PD-1 (37). Because these different works did not fully integrate in their analysis, the impact of coexisting mutations, different proportions of *STK11* and/or *EGFR* alterations in *TP53* or *KRAS* mutated tumors in each study could again explain the contradictory results obtained. Indeed, the work of Dong and colleagues also used the Rizvi cohort in which half of the *KRAS*-mutated patients belonged to the *TP53*-Mut/*STK11-EGFR*-WT tumor group, while only one patient belonged to the $STK11_{(or)}$-*EGFR*-Mut tumor group (18). Moreover, in the CERTIM cohort, *KRAS* mutations were not associated with a longer survival probably because no tumors with *KRAS* alterations belonged to the *TP53*-Mut/*STK11-EGFR*-WT tumor group. Thus, the impact of *KRAS* mutations on the response to anti–PD-1 might be rather linked to co-occurring alterations than to a direct impact of this mutation. In agreement, our study strongly suggested that *KRAS* mutation did not significantly affect the response to PD-1 blockers in patients harboring a *TP53-STK11-EGFR*-WT tumor, nor a *STK11*-Mut/*EGFR-TP53*-WT tumor. Nevertheless, studies involving higher numbers of anti–PD-1 treated patients are needed to determine whether an additional *KRAS* mutation may affect patients' survival in the group of *TP53*-Mut/*STK11-EGFR*-WT tumors.

Finally, patients with *TP53-STK11-EGFR*-WT tumors, including those with *KRAS* mutations, seemed to have an intermediate response (OS) to nivolumab in the CERTIM cohort. Additional markers to identify responders in this last group will probably be mandatory. In *KRAS* mutants, comutations in *KEAP1*/*NFE2L2* were recently shown to be associated with reduced survival in patients treated with PD-1 inhibitors (37), while the presence of EML4–ALK fusion gene was associated with a higher expression level of PD-L1 in NSCLC (39). Regarding p53, its function can be lost independently of *TP53* mutations, through genetic or epigenetic alterations of p16INK4 that can lead to the loss of $p14^{ARF}$ (40, 41). Because $p14^{ARF}$ is an inhibitor of mdm2, an ubiquitin-protein ligase promoting p53 degradation, the loss of $p14^{ARF}$ indirectly promotes p53 degradation. Consequently, additional studies are mandatory to investigate the potential impact of the loss of p53 function, which occurred independently of *TP53* mutations, on the immune profile of tumors. Overall, some additional gene rearrangements, genetic or epigenetic alterations might be helpful to distinguish even more precisely responders among nonresponders in anti–PD-1-treated patients.

The originality of our work relies on the fact that we investigated the impact of each distinct combination of mutations on the TIP. This methodology showed that the evaluation of different combinations of *TP53*, *EGFR*, and *STK11* mutations had a superior capacity to predict TIPs and the response to anti–PD-1 than that of each individual mutation. It leads us to reveal that the presence of *TP53* mutations without alterations of *STK11* and of *EGFR* was associated with a longer survival in anti–PD-1-treated patients. Moreover, our results suggested that the predictive potential of PD-L1 expression on the response to PD-1 blockers was restricted to *TP53*-Mut/*STK11-EGFR*-WT tumors and thus could provide an additional signal to better identify patients with long-term responses. It should be noted that one of the limitations of our study was that we did not compare the performance of the combinations of *TP53*/*EGFR*/*STK11* mutations to predict the response to PD-1 blockers to that of the TIPs. Indeed, as opposed to the 221 untreated lung adenocarcinoma cohort, in the CERTIM cohort, patients did not benefit from complete surgical resection, and only small tumor biopsies were available for analysis. Consequently, exhaustive immune cell characterization was not possible and not reliable for these patients. A potential additional limitation was that the anti–PD-L1 antibodies used to perform IHC experiments were not the same in the CERTIM (E1L3N) and the Rizvi cohort (22C3). However, our recent work (42) and another study (43) indicated that these two antibodies appeared to be interchangeable from an analytic perspective.

Finally, by deciphering the immune network of lung adenocarcinoma, this study provided evidence that routine NGS testing common mutations, associated with the level of PD-L1 expression by tumor cells, represent robust biomarkers to identify best responders to PD-1 blockade.

Disclosure of Potential Conflicts of Interest

N. Pécuchet is an employee of Dassault Systemes. F. Goldwasser is a consultant/advisory board member for Baxter and Fresenius Kabi. P. Laurent-Puig is a consultant/advisory board member for Amgen, AstraZeneca, Biocartis, Boerhinger Ingelheim, Bristol-Myers Squibb, Merck Serono, MSD, and Roche. M.-C. Dieu-Nosjean reports receiving commercial research grants from AstraZeneca and Janssen, and speakers bureau honoraria from Bristol-Myers Squibb, Merck, and MSD. No potential conflicts of interest were disclosed by the other authors.

Authors' Contributions

Conception and design: J. Biton, P. Laurent-Puig, M-C. Dieu-Nosjean, R. Herbst, H. Blons, D. Damotte

Development of methodology: J. Biton, A. Mansuet-Lupo, M. Alifano, P. Laurent-Puig, M-C. Dieu-Nosjean, H. Blons, D. Damotte

Acquisition of data (provided animals, acquired and managed patients, provided facilities, etc.): J. Biton, A. Mansuet-Lupo, N. Pécuchet, M. Alifano, H. Ouakrim, J. Arrondeau, P. Boudou-Rouquette, F. Goldwasser, K. Leroy, J. Goc, C. Germain, P. Laurent-Puig, M-C. Dieu-Nosjean, H. Blons, D. Damotte

Analysis and interpretation of data (e.g., statistical analysis, biostatistics, computational analysis): J. Biton, A. Mansuet-Lupo, N. Pécuchet, H. Ouakrim, F. Goldwasser, M. Wislez, P. Laurent-Puig, M-C. Dieu-Nosjean, D. Damotte

Writing, review, and/or revision of the manuscript: J. Biton, A. Mansuet-Lupo, N. Pécuchet, M. Alifano, J. Arrondeau, P. Boudou-Rouquette, F. Goldwasser, K. Leroy, J. Goc, M. Wislez, C. Germain, P. Laurent-Puig, M-C. Dieu-Nosjean, I. Cremer, R. Herbst, H. Blons, D. Damotte

Administrative, technical, or material support (i.e., reporting or organizing data, constructing databases): J. Biton, A. Mansuet-Lupo, N. Pécuchet, H. Ouakrim, J. Goc, D. Damotte

Study supervision: J. Biton, F. Goldwasser, D. Damotte

Acknowledgments

This work was supported by the Institut National de la Santé et de la Recherche Médicale (INSERM), Paris Descartes-Paris 5 University, Pierre et Marie Curie-Paris 6 University, the Cancer Research for Personalized Medicine

Downloaded from http://aacrjournals.org/clincancerres/article-pdf/24/22/5710/2049288/5710.pdf by guest on 10 January 2023

(CARPEM), the LabEx Immuno-oncology, the Institut National du Cancer (2011-PLBIO-06-INSERM 6-1), and MedImmune.

The authors thank Patricia Bonjour, Béatrice Marmey (Department of Pathology, Hôpital Cochin, Paris), Sarah Leseurre (Department of Thoracic Surgery, Hôpital Cochin, Paris), and Nathalie Jupiter and Samantha Knockaert (UMRS 1138, Cordeliers Research Center, Team 13, Paris) for technical assistance.

The costs of publication of this article were defrayed in part by the payment of page charges. This article must therefore be hereby marked *advertisement* in accordance with 18 U.S.C. Section 1734 solely to indicate this fact.

Received January 18, 2018; revised March 14, 2018; accepted May 10, 2018; published first May 15, 2018.

References

1. Topalian SL, Hodi FS, Brahmer JR, Gettinger SN, Smith DC, McDermott DF, et al. Safety, activity, and immune correlates of anti-PD-1 antibody in cancer. N Engl J Med 2012;366:2443–54.
2. Robert C, Schachter J, Long GV, Arance A, Grob JJ, Mortier L, et al. Pembrolizumab versus ipilimumab in advanced melanoma. N Engl J Med 2015;372:2521–32.
3. Motzer RJ, Escudier B, McDermott DF, George S, Hammers HJ, Srinivas S, et al. Nivolumab versus everolimus in advanced renal-cell carcinoma. N Engl J Med 2015;373:1803–13.
4. Borghaei H, Paz-Ares L, Horn L, Spigel DR, Steins M, Ready NE, et al. Nivolumab versus docetaxel in advanced nonsquamous non-small-cell lung cancer. N Engl J Med 2015;373:1627–39.
5. Reck M, Rodríguez-Abreu D, Robinson AG, Hui R, Csőszi T, Fülöp A, et al. Pembrolizumab versus chemotherapy for PD-L1-positive non-small-cell lung cancer. N Engl J Med 2016;375:1823–33.
6. Rizvi NA, Hellmann MD, Snyder A, Kvistborg P, Makarov V, Havel JJ, et al. Cancer immunology. Mutational landscape determines sensitivity to PD-1 blockade in non-small cell lung cancer. Science 2015;348:124–8.
7. Le DT, Durham JN, Smith KN, Wang H, Bartlett BR, Aulakh LK, et al. Mismatch repair deficiency predicts response of solid tumors to PD-1 blockade. Science 2017;357:409–13.
8. Mazzaschi G, Madeddu D, Falco A, Bocchialini G, Goldoni M, Sogni F, et al. Low PD-1 expression in cytotoxic CD8+ tumor-infiltrating lymphocytes confers an immune-privileged tissue microenvironment in NSCLC with a prognostic and predictive value. Clin Cancer Res 2018; 24:407–19.
9. Prat A, Navarro A, Paré L, Reguart N, Galván P, Pascual T, et al. Immune-related gene expression profiling after PD-1 blockade in non-small cell lung carcinoma, head and neck squamous cell carcinoma, and melanoma. Cancer Res 2017;77:3540–50.
10. Ock C-Y, Keam B, Kim S, Lee J-S, Kim M, Kim TM, et al. Pan-cancer immunogenomic perspective on the tumor microenvironment based on PD-L1 and CD8 T-cell infiltration. Clin Cancer Res 2016;22:2261–70.
11. Campesato LF, Barroso-Sousa R, Jimenez L, Correa BR, Sabbaga J, Hoff PM, et al. Comprehensive cancer-gene panels can be used to estimate mutational load and predict clinical benefit to PD-1 blockade in clinical practice. Oncotarget 2015;6:34221–7.
12. Johnson DB, Frampton GM, Rioth MJ, Yusko E, Xu Y, Guo X, et al. Targeted next generation sequencing identifies markers of response to PD-1 blockade. Cancer Immunol Res 2016;4:959–67.
13. Xu C, Fillmore CM, Koyama S, Wu H, Zhao Y, Chen Z, et al. Loss of Lkb1 and Pten leads to lung squamous cell carcinoma with elevated PD-L1 expression. Cancer Cell 2014;25:590–604.
14. Mandai M, Hamanishi J, Abiko K, Matsumura N, Baba T, Konishi I. Dual faces of IFNγ in cancer progression: a role of PD-L1 induction in the determination of pro- and antitumor immunity. Clin Cancer Res 2016;22: 2329–34.
15. Skoulidis F, Byers LA, Diao L, Papadimitrakopoulou VA, Tong P, Izzo J, et al. Co-occurring genomic alterations define major subsets of KRAS-mutant lung adenocarcinoma with distinct biology, immune profiles, and therapeutic vulnerabilities. Cancer Discov 2015;5:860–77.
16. Cortez MA, Ivan C, Valdecanas D, Wang X, Peltier HJ, Ye Y, et al. PDL1 regulation by p53 via miR-34. J Natl Cancer Inst 2016;108:303–13.
17. Ji M, Liu Y, Li Q, Li X, Ning Z, Zhao W, et al. PD-1/PD-L1 expression in non-small-cell lung cancer and its correlation with EGFR/KRAS mutations. Cancer Biol Ther 2016;17:407–13.
18. Dong Z-Y, Zhong W-Z, Zhang X-C, Su J, Xie Z, Liu S-Y, et al. Potential predictive value of TP53 and KRAS mutation status for response to PD-1 blockade immunotherapy in lung adenocarcinoma. Clin Cancer Res 2017;23:3012–24.
19. Mansuet-Lupo A, Alifano M, Pécuchet N, Biton J, Becht E, Goc J, et al. Intratumoral immune cell densities are associated with lung adenocarcinoma gene alterations. Am J Respir Crit Care Med 2016;194: 1403–12.
20. Goc J, Germain C, Vo-Bourgais TKD, Lupo A, Klein C, Knockaert S, et al. Dendritic cells in tumor-associated tertiary lymphoid structures signal a Th1 cytotoxic immune contexture and license the positive prognostic value of infiltrating CD8+ T cells. Cancer Res 2014;74: 705–15.
21. de Chaisemartin L, Goc J, Damotte D, Validire P, Magdeleinat P, Alifano M, et al. Characterization of chemokines and adhesion molecules associated with T cell presence in tertiary lymphoid structures in human lung cancer. Cancer Res 2011;71:6391–9.
22. Dieu-Nosjean M-C, Goc J, Giraldo NA, Sautès-Fridman C, Fridman WH. Tertiary lymphoid structures in cancer and beyond. Trends Immunol 2014;35:571–80.
23. Cancer Genome Atlas Research Network. Comprehensive molecular profiling of lung adenocarcinoma. Nature 2014;511:543–50.
24. Kato S, Han S-Y, Liu W, Otsuka K, Shibata H, Kanamaru R, et al. Understanding the function-structure and function-mutation relationships of p53 tumor suppressor protein by high-resolution missense mutation analysis. Proc Natl Acad Sci U S A 2003;100:8424–9.
25. Kobayashi Y, Togashi Y, Yatabe Y, Mizuuchi H, Jangchul P, Kondo C, et al. EGFR exon 18 mutations in lung cancer: molecular predictors of augmented sensitivity to afatinib or neratinib as compared with first- or third-generation TKIs. Clin Cancer Res 2015;21:5305–13.
26. Pécuchet N, Laurent-Puig P, Mansuet-Lupo A, Legras A, Alifano M, Pallier K, et al. Different prognostic impact of STK11 mutations in non-squamous non-small-cell lung cancer. Oncotarget 2017;8:23831–40.
27. Dearden S, Stevens J, Wu Y-L, Blowers D. Mutation incidence and coincidence in non small-cell lung cancer: meta-analyses by ethnicity and histology (mutMap). Ann Oncol 2013;24:2371–6.
28. Parsa AT, Waldron JS, Panner A, Crane CA, Parney IF, Barry JJ, et al. Loss of tumor suppressor PTEN function increases B7-H1 expression and immunoresistance in glioma. Nat Med 2007;13:84–8.
29. Biton J, Ouakrim H, Dechartres A, Alifano M, Mansuet-Lupo A, Si H, et al. Impaired tumor-infiltrating T cells in patients with COPD impacts lung cancer response to PD-1 blockade. Am J Respir Crit Care Med 2018 Mar 8 [Epub ahead of print].
30. Koyama S, Akbay EA, Li YY, Aref AR, Skoulidis F, Herter-Sprie GS, et al. STK11/LKB1 deficiency promotes neutrophil recruitment and proinflammatory cytokine production to suppress T-cell activity in the lung tumor microenvironment. Cancer Res 2016;76:999–1008.
31. Terawaki S, Chikuma S, Shibayama S, Hayashi T, Yoshida T, Okazaki T, et al. IFN-α directly promotes programmed cell death-1 transcription and limits the duration of T cell-mediated immunity. J Immunol 2011;186: 2772–9.
32. Marchetti A, Martella C, Felicioni L, Barassi F, Salvatore S, Chella A, et al. EGFR mutations in non-small-cell lung cancer: analysis of a large series of cases and development of a rapid and sensitive method for diagnostic screening with potential implications on pharmacologic treatment. J Clin Oncol 2005;23:857–65.
33. Schabath MB, Welsh EA, Fulp WJ, Chen L, Teer JK, Thompson ZJ, et al. Differential association of STK11 and TP53 with KRAS mutation-associated gene expression, proliferation and immune surveillance in lung adenocarcinoma. Oncogene 2016;35:3209–16.
34. Chen N, Fang W, Zhan J, Hong S, Tang Y, Kang S, et al. Upregulation of PD-L1 by EGFR activation mediates the immune escape in EGFR-driven NSCLC: implication for optional immune targeted therapy for NSCLC patients with EGFR mutation. J Thorac Oncol 2015;10:910–23.

Downloaded from http://aacrjournals.org/clincancerres/article-pdf/24/22/5710/2049288/5710.pdf by guest on 10 January 2023

35. Riely GJ, Marks J, Pao W. KRAS mutations in non-small cell lung cancer. Proc Am Thorac Soc 2009;6:201–5.
36. Gainor JF, Shaw AT, Sequist LV, Fu X, Azzoli CG, Piotrowska Z, et al. EGFR mutations and ALK rearrangements are associated with low response rates to PD-1 pathway blockade in non-small cell lung cancer: a retrospective analysis. Clin Cancer Res 2016;22:4585–93.
37. Arbour KC, Jordan EJ, Kim HR, Dienstag J, Yu H, Sanchez-Vega F, et al. Effects of co-occurring genomic alterations on outcomes in patients with *KRAS*-mutant non-small cell lung cancer. Clin Cancer Res 2018; 24:334–40.
38. Lee CK, Man J, Lord S, Cooper W, Links M, Gebski V, et al. Clinical and molecular characteristics associated with survival among patients treated with checkpoint inhibitors for advanced non-small cell lung carcinoma: a systematic review and meta-analysis. JAMA Oncol 2018;4:210–6.
39. Ota K, Azuma K, Kawahara A, Hattori S, Iwama E, Tanizaki J, et al. Induction of PD-L1 expression by the EML4-ALK oncoprotein and downstream signaling pathways in non-small cell lung cancer. Clin Cancer Res 2015;21:4014–21.
40. Pomerantz J, Schreiber-Agus N, Liégeois NJ, Silverman A, Alland L, Chin L, et al. The Ink4a tumor suppressor gene product, p19Arf, interacts with MDM2 and neutralizes MDM2's inhibition of p53. Cell 1998;92: 713–23.
41. Bates S, Phillips AC, Clark PA, Stott F, Peters G, Ludwig RL, et al. $p14^{ARF}$ links the tumour suppressors RB and p53. Nature 1998;395:124–5.
42. Rimm DL, Han G, Taube JM, Yi ES, Bridge JA, Flieder DB, et al. A Prospective, multi-institutional, pathologist-based assessment of 4 immunohistochemistry assays for PD-L1 expression in non-small cell lung cancer. JAMA Oncol 2017;3:1051–8.
43. Adam J, Le Stang N, Rouquette I, Cazes A, Badoual C, Pinot-Roussel H, et al. Multicenter French harmonization study for PD-L1 IHC testing in non-small cell lung cancer. Ann Oncol [cited 2018 Jan 17]; Available from: https://academic.oup.com/annonc/advance-article/doi/10.1093/annonc/mdy014/4812668

Downloaded from http://aacrjournals.org/clincancerres/article-pdf/24/22/5710/2049288/5710.pdf by guest on 10 January 2023